Cancer Immunology, Immunotherapy (2018) 67:1491–1503
https://doi.org/10.1007/s00262-018-2184-2

ORIGINAL ARTICLE

Absence of host NF-κB p50 induces murine glioblastoma tumor regression, increases survival, and decreases T-cell induction of tumor-associated macrophage M2 polarization

Theresa Barberi[1] · Allison Martin[1] · Rahul Suresh[1] · David J. Barakat[1] · Sarah Harris-Bookman[1] · Charles G. Drake[1] · Michael Lim[1] · Alan D. Friedman[1]

Received: 20 December 2017 / Accepted: 7 June 2018 / Published online: 21 July 2018

Abstract

High-grade gliomas harbor abundant myeloid cells that suppress anti-tumor immunity and support tumor growth. Targeting transcription factors, such as NF-κB p50, that mediate suppressive myeloid M2 polarization may prove therapeutic. GL261-Luc glioblastoma cells were inoculated into wild-type and $p50^{-/-}$ mice, followed by analysis of tumor growth, survival, tumor myeloid cells, and T cells. The absence of host p50 slows tumor growth and enables regression in 30% of recipients, leading to prolonged survival. Tumors developing in $p50^{-/-}$ mice possess a greater concentration of tumor-infiltrating myeloid cells (TIMs) than those in wild-type mice. TIMs are predominantly $F4/80^{hi}$ macrophages which, along with tumor-associated microglia, express increased pro-inflammatory M1 and reduced immune-suppressive M2 markers. In $p50^{-/-}$ mice, total tumor CD4 T cells are threefold more abundant, whereas CD8 T-cell numbers are unchanged, and both produce increased IFNγ and Granzyme B. Naïve splenic $p50^{-/-}$ CD8 T cells manifest increased activation, whereas naïve $p50^{-/-}$ and WT CD4 T cells show similar Th1, Th2, and Th17 polarization. Antibody targeting CD4, but not CD8, fully obviates the $p50^{-/-}$ survival advantage. Combined CD4 and CD8 T-cell depletion reverses myeloid M2 polarization in wild-type hosts, without affecting myeloid M1 polarization in $p50^{-/-}$ hosts. Finally, gliomas grow similarly in p50(f/f) and p50(f/f);Lysozyme-Cre mice, the latter having reduced p50 specifically in myeloid cells and tumor microglia. Thus, high-grade glioma T cells play a key role in directing M2 polarization of tumor myeloid cells, and reducing NF-κB p50 in both tumor myeloid cells and T cells may contribute to glioma therapy.

Keywords Glioblastoma · Macrophages · NF-κB p50 · T cells · Immunotherapy

Abbreviations

B6	C57BL/6
BMDM	Bone-marrow-derived macrophage
FC	Flow cytometry
GBM	Glioblastoma
IVIS	In vivo imaging system
MR	Mannose receptor
p50	NF-κB p50
PBS	Phosphate-buffered saline
qRT-PCR	Quantitative real-time PCR
TAM	Tumor-associated macrophage
TIM	Tumor-infiltrating myeloid cell
WT	Wild type

Introduction

Glioblastoma (GBM) is a uniformly fatal brain tumor. The microenvironment of high-grade gliomas contains an abundance of myeloid cells, which comprise as much as 40% of the tumor [1, 2]. Glioma myeloid cells broadly fall into two categories: (1) brain-resident microglia, which derive from embryonic macrophages and are present in the healthy brain and (2) tumor-infiltrating myeloid cells (TIM) that are derived from blood monocytes and granulocytes and are recruited to the brain under pathological conditions [3, 4].

Electronic supplementary material The online version of this article (https://doi.org/10.1007/s00262-018-2184-2) contains supplementary material, which is available to authorized users.

✉ Alan D. Friedman
afriedm2@jhmi.edu

[1] Division of Pediatric Oncology, Department of Oncology, Johns Hopkins University, CRB I, Rm 253, 1650 Orleans St., Baltimore, MD 21231, USA

Blood monocytes can mature into tumor-associated macrophages (TAMs); in addition, TIM can retain a more immature phenotype and be classified further into granulocytic or monocytic MDSC [5–9]. Gliomas produce cytokines such as CSF1 that polarize TAMs and microglia towards the immune-suppressive, tumor-supportive M2, as opposed to the pro-inflammatory M1 phenotype [1, 10]. M2 TAM also support tumor growth by producing proangiogenic, proliferative, and invasive factors.

Due to their abundance and ability to influence T-cell function, glioma myeloid cells represent a potential therapeutic target. Supporting the utility of tumor myeloid reprogramming, inhibiting the tyrosine kinase activity of the CSF1 receptor alters TAM in a PDGF;*Cdkn2a*$^{-/-}$ murine glioma model by reducing M2 and increasing M1 markers, leading to prolonged survival. The same agent slows growth of human GBM in NOD/SCID mice [11]. However, gliomas secrete additional cytokines capable of inducing M2 polarization, including GM-CSF and IL-4, ultimately enabling outgrowth of CSF1R inhibitor-resistant gliomas [12, 13].

CSF1, GM-CSF, and IL-4 signaling may converge on common transcription factors to favor M2 gene expression. Transcription factors contributing to M2 macrophage polarization include NF-κB p50 (p50), C/EBPβ, KLF4, STAT6, PPARγ, and RORC1 [14–23]. Melanoma and fibrosarcoma cells grow more slowly in p50$^{-/-}$ compared with wild-type (WT) hosts, and also in WT hosts transplanted with p50$^{-/-}$ compared with WT marrow [15], but detailed characterization of the cellular mechanisms responsible for slowed tumor growth is lacking. We add to the existing literature by investigating the contribution of host p50 to the growth of glioma, a tumor that arises in a unique microenvironment. We find that intracranial GL261 glioma cells grow more slowly in p50$^{-/-}$ mice and exhibit striking tumor regression in a subset of these mice, with prolonged survival. We have characterized changes in the glioma immune microenvironment associated with this dramatic phenotype and demonstrate not only macrophage and microglia reprogramming, but also a previously unappreciated role for T cells in directing this process. In addition, we show that glioma growth is unimpaired in a novel mouse model lacking p50 specifically in macrophages, activated monocytes, and granulocytes. We conclude that targeting NF-κB p50 in T cells, or in both T cells and myeloid cells, may provide an effective glioma immunotherapy.

Materials and methods

Tumor inoculation, imaging, and survival analysis

GL261-Luc cells [24] were grown in DMEM with 10% FBS. They were inoculated intra-cranially into the striatum as described [25]. For tumor imaging, mice were injected with luciferin (100 µg/g i.p.) in PBS; after 10 min the mice were anesthetized using isofluorane-O_2 gas and imaged using the Spectrum (Perkin Elmer) in vivo imaging system (IVIS). To deplete CD4 or CD8 T cells, WT and p50$^{-/-}$ mice were administered rat-anti-CD4 or CD8 antibodies (Bio-X-Cell) i.p.

Tumor myeloid and T-cell isolation

Mice anesthetized with ketamine and xylazine were perfused with ice-cold PBS at 7 mL/min for 8 min via their exposed left ventricle using a syringe pump. Brains were removed from euthanized mice and placed in calcium/magnesium-free HBSS. Enzymatic cell dissociation was accomplished using Neural Tissue Dissociation Kit P (Miltenyi), following the protocol for the Octo Dissociator, program 37C_ABDK. HBSS with 1.26 mM $CaCl_2$, 0.5 mM $MgCl_2$, and 0.4 mM $MgSO_4$ was then added, followed by passage through a 40 µm cell strainer and centrifugation at 300×*g* for 5 min. The pellet was resuspended in 7 mL 30% isotonic Percoll in PBS and centrifuged at room temperature for 10 min at 700×*g*. The top myelin layer and Percoll were aspirated, and the cell pellet was washed with MACS buffer (Miltenyi). Cells were then either stained for flow cytometry (FC), or separated into CD11b$^+$ and CD11b$^-$ or CD3$^+$ and CD3$^-$ cell fractions using CD11b or CD3 positive selection kits and LS columns (Miltenyi).

Tumor myeloid and T-cell subset and activation analyses

All antibody staining was preceded by 15 min of 1:50 FcγR block in FC buffer, on ice. Extracellular antibodies were then added to FC buffer containing FcγR block, and incubated for 45 min on ice. Intracellular staining was accomplished after surface staining using the Foxp3 staining kit (eBioscience). Myeloid subsets were stained with anti-CD11b-FITC, anti-Ly6C-AF700, anti-MR-PE-Cy7, anti-CD11c-PE/Dazzle594, anti-Ly6G-BV605 (BioLegend), anti-MHCII-eFluor450 (eBioscience), and anti-F4/80-APC (BioRad). To evaluate Tregs, cells were stained with anti-CD3-AF488, anti-CD4-APC, anti-CD25-PerCP-Cy5.5 (BioLegend), and anti-Foxp3-PE (BD Pharmingen). To assess T-cell activation, total tumor cells were incubated for 4 h at 37 °C in a 5% CO_2 incubator with Protein Transport Inhibitor Cocktail containing brefeldin A and monensin, or with Cell Stimulation Cocktail containing protein transport inhibitors and PMA/ionomycin (eBioscience). Cells were then stained with anti-CD3-AF488, anti-CD4-PE, and anti-CD8-PerCP-Cy5.5 followed by intracellular stain with anti-IFNγ-APC (BioLegend). In addition, 1E5 CD3$^+$ cells were stimulated with 4E4 CD3/CD28 Dynabeads (ThermoFisher) for 3 days, followed

by staining using anti-CD3-PerCP-Cy5.5, anti-CD8-BV650, anti-CD4-BV605, anti-IFNγ-APC, anti-TNFα-BV421 (BioLegend), and anti-GranzymeB-PE (eBioscience).

Naïve splenic T-cell analysis

To obtain naïve CD4 T cells, spleens were passed through a cell strainer, subjected to red cell lysis, and selected using a CD8 positive selection kit (Miltenyi). $CD8^-$ cells were then subjected to negative selection using a naïve CD4 T-cell isolation kit (Miltenyi). The cells bound to the column included APC. To obtain naïve CD8 T cells, splenocytes were subjected to selection using the Pan T-cell isolation kit II (Miltenyi), yielding $CD3^+$ T cells and the bound $CD3^-$ fraction that includes APCs. The $CD3^+$ cells were then further processed using a naïve CD8α T-cell isolation kit (Miltenyi). Naïve T cells were combined with irradiated (3000 cGy) APCs and cultured with different cytokine and antibody combinations to favor lineage polarization, plus anti-CD3 antibody, followed by PMA/ionomycin stimulation and FC analysis [26].

Bone-marrow-derived myeloid cells and peritoneal macrophages

To obtain bone-marrow-derived macrophages (BMDM), marrow was cultured on bacterial dishes with DMEM, 10% heat-inactivated FBS, and CSF1 (20 ng/ml) for 7 days, followed by stimulation of adherent cells with IL-4 (20 ng/ml) or IFNγ (20 ng/ml) or vehicle for 24 h. To isolate peritoneal macrophages, 10 ml of ice-cold HBSS was inserted into the peritoneal cavity and removed. Cells were resuspended in DMEM with 10% heat-inactivated FBS and transferred to a tissue culture plate overnight.

RNA, DNA, and western blot analyses

RNA was isolated using NucleoSpin RNA II (Machery-Nagel). First-strand cDNA was prepared using AMV reverse transcriptase (Promega) and oligodT. Quantitative real-time PCR (qRT-PCR) was carried out using Lo-Rox SYBR Green (Alkali Scientific). Primers are listed (Supplementary Table S1). Genomic DNA from p50(f/f) and p50(f/f);Lys-Cre BMDM was PCR amplified using intron 3 primer 5′-CACAAGTGTGTGGAGGCTGAAGG-3′ and intron 4 primer 5′-ACTTTCCTACTGTTTCCCCAGAGCC-3′, followed by agarose gel electrophoresis and ethidium bromide staining. Total cellular proteins prepared in Laemmli sample buffer were subjected to Western blotting using p50 (13586, Cell Signaling) and β-actin (AC-15, Sigma) antibodies.

Data analysis

Survival curves were compared using the log rank test. Tumor bioluminescence, myeloid and T-cell subsets, and RNA expression values were compared using the Student *t* test. Means and SEs are shown.

Results

Absence of NF-κB p50 slows GL261 glioma growth and prolongs survival

GL261 cells, derived from a B6 mouse by chemical mutagenesis, are widely used as a glioma model. These cells closely mimic human GBM angiogenesis and invasiveness and contain abundant M2 TAMs [24]. WT or $p50^{-/-}$ mice were implanted with GL261-Luc cells and assessed weekly by IVIS to track tumor growth. Representative images for WT and $p50^{-/-}$ recipients are shown (Fig. 1a, left). We found that 12 of the 39 tumors in $p50^{-/-}$ hosts that were detectable on day 14 subsequently regressed, as illustrated by the second $p50^{-/-}$ mouse. In contrast, only 1 of 43 such tumors in WT mice regressed (Fig. 1a, right). $p50^{-/-}$ tumor recipients had significantly prolonged survival compared with WT recipients (Fig. 1b), with a trend toward reduced tumor size on day 14 and a significant, > threefold reduction in tumor size on day 21 (Fig. 1c). The day 21 data underestimates the difference in tumor sizes, as 11 WT recipients died prior to day 21 imaging.

Characterization of glioma-associated myeloid cells

Previous studies demonstrate that tumors harbor $F4/80^{hi}Ly6C^{int/lo}MHCII^{hi/lo}$ macrophages, $F4/80^{lo}Ly6C^{hi}MHCII^{lo}$ monocytes, and $Ly6G^+$ granulocytes, the latter two subsets potentially representing monocytic or granulocytic MDSCs [27–29]. We sought to characterize GL261 glioma-associated myeloid cells. CD11b is a pan-myeloid marker. Microglia can be partially resolved from other myeloid populations by their low/intermediate expression of CD45 [27, 30]. FC demonstrates abundant $CD45^{int}CD11b^{int}$ microglia in healthy tumor-free brains, but very few $CD45^{hi}CD11b^{hi}$ cells (less than 0.5% of total cells and 8% of $CD45^+$ cells, on average, $n=3$, not shown). In WT and $p50^{-/-}$ tumor-bearing mice, we observe a large increase in $CD45^{hi}CD11b^{hi}$ cells, which we denote tumor-infiltrating myeloid cells or TIMs (Fig. 2a, left). TIMs comprise about 40%, and microglia 45%, of $CD45^+$ cells in both WT and $p50^{-/-}$ tumor-bearing brains (Fig. 2a, center), with $CD45^+$ cells representing ~50% of total cells (not shown). Since substantial TIM accumulation only occurs in the presence of tumor but not in healthy brain, we approximated TIM

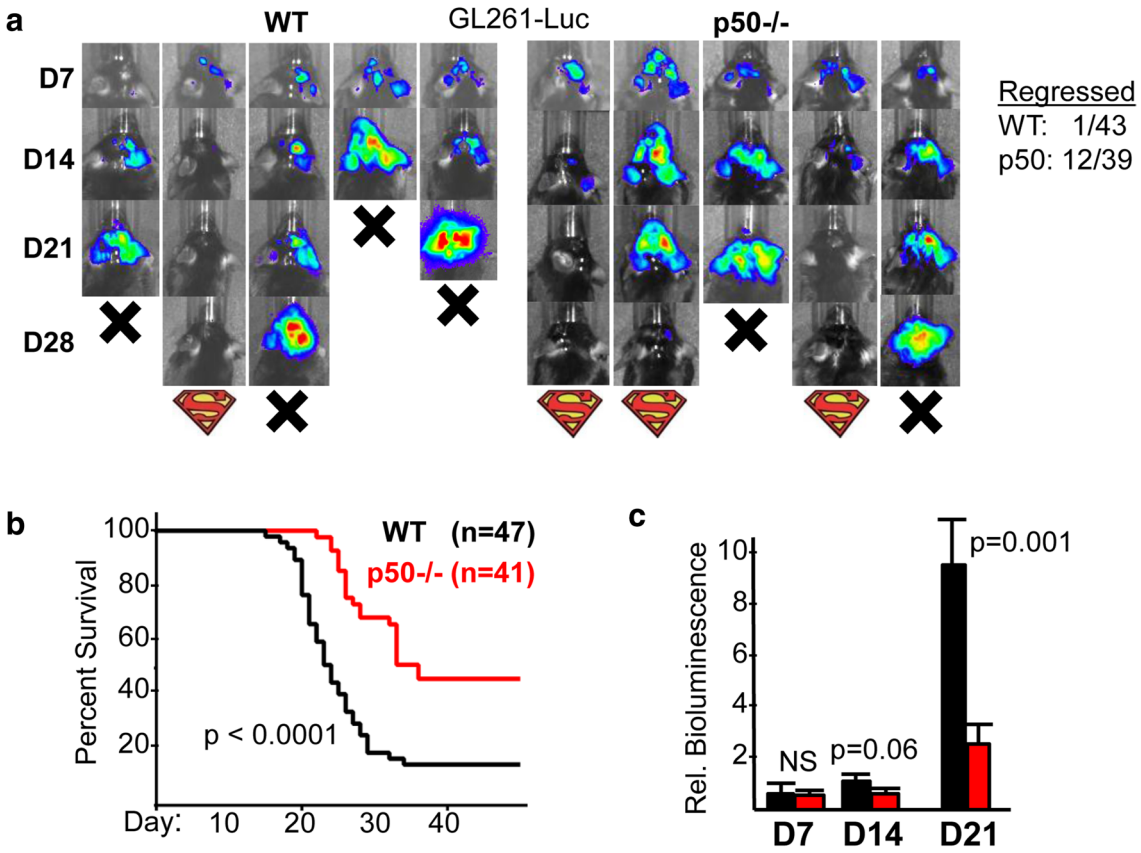

Fig. 1 Glioma growth is slowed in mice lacking NF-κB p50. **a** Representative IVIS images on days 7, 14, and 21 after GL261-Luc inoculation into WT or $p50^{-/-}$ recipients (left). Mice dead on the indicated days are denoted as X, and those that showed prolonged survival with the Superman logo. Also shown (right) are the numbers of WT and $p50^{-/-}$ mice that were $IVIS^{+}$ on day 14 and later demonstrated tumor regression. **b** Survival curves of WT vs $p50^{-/-}$ mice inoculated on day 0 with GL261-Luc cells, with total number of mice in each group and Log Rank *p* values shown. **c** Relative IVIS bioluminescence of tumors on days 7, 14, and 21 from the same mice used for survival analysis. Mean, SE, and *p* values are shown. *NS* Not significant

density by dividing the total TIM number by tumor bioluminescence for each mouse, revealing a ~threefold increase in TIM density in $p50^{-/-}$ hosts (Fig. 2a, right). 80–84% of TIMs are $F4/80^{hi}$, and 70–78% are $MHCII^{hi}$ (Fig. 2b). $Ly6G^{+}$ cells represent only 1–2% of $CD45^{+}$ cells (Fig. 2c). Ly6C and MHCII staining has previously been used to subdivide TIM subsets, with $Ly6C^{int}MHCII^{hi}$ cells correlating with reduced tumor growth [28, 29, 31]. As we perfused mice with PBS prior to brain isolation, we detect few tumor-associated $Ly6C^{hi}$ monocytes (Supplementary Fig. 1a), but do find $Ly6C^{int}$ and $Ly6C^{lo}$ cells with varying expression of MHCII, as seen in a representative FC plot (Fig. 2d, left); these uniformly express the F4/80 macrophage marker (Supplementary Fig. 1b). When cells are gated into four quadrants as $Ly6C^{int}MHCII^{lo}$, $Ly6C^{int}MHCII^{hi}$, $Ly6C^{lo}MHCII^{hi}$, and $Ly6C^{lo}MHCII^{lo}$, we find nearly a twofold increase in the frequency of $Ly6C^{int}MHCII^{hi}$ TIMs in $p50^{-/-}$ compared to WT tumor-bearing mice, making this the most predominant TIM population (Fig. 2d, right). When normalized to tumor size using bioluminescence, we observe a fourfold increase in the density of $Ly6C^{int}MHCII^{hi}$ TIMs, and no change in the density of $Ly6C^{lo}MHCII^{hi}$ TIMs, in $p50^{-/-}$ mice (not shown). In a rat glioma model, $CD11c^{hi}$ macrophages potentiated orthotopic tumor growth [32]. Consistent with reduced tumor growth, CD11c expression was decreased in the predominant $Ly6C^{int}MHCII^{hi}$ TIM subset, but was unchanged in the other three Ly6C;MHCII populations in $p50^{-/-}$ hosts (Fig. 2e).

Absence of NF-κB p50 favors a pro-inflammatory M1 TIM phenotype

The frequency of TIMs expressing MHCII was increased and of those expressing the M2 marker mannose receptor (MR) decreased in $p50^{-/-}$ compared with WT tumor recipients (Fig. 3a, left). The density of $MHCII^{hi}$ TIMs and MR^{-} TIMs were both increased in $p50^{-/-}$ mice (Fig. 3a, right). We further found that MR expression was decreased in all four $p50^{-/-}$ TIM Ly6C;MHCII subsets (Fig. 3b).

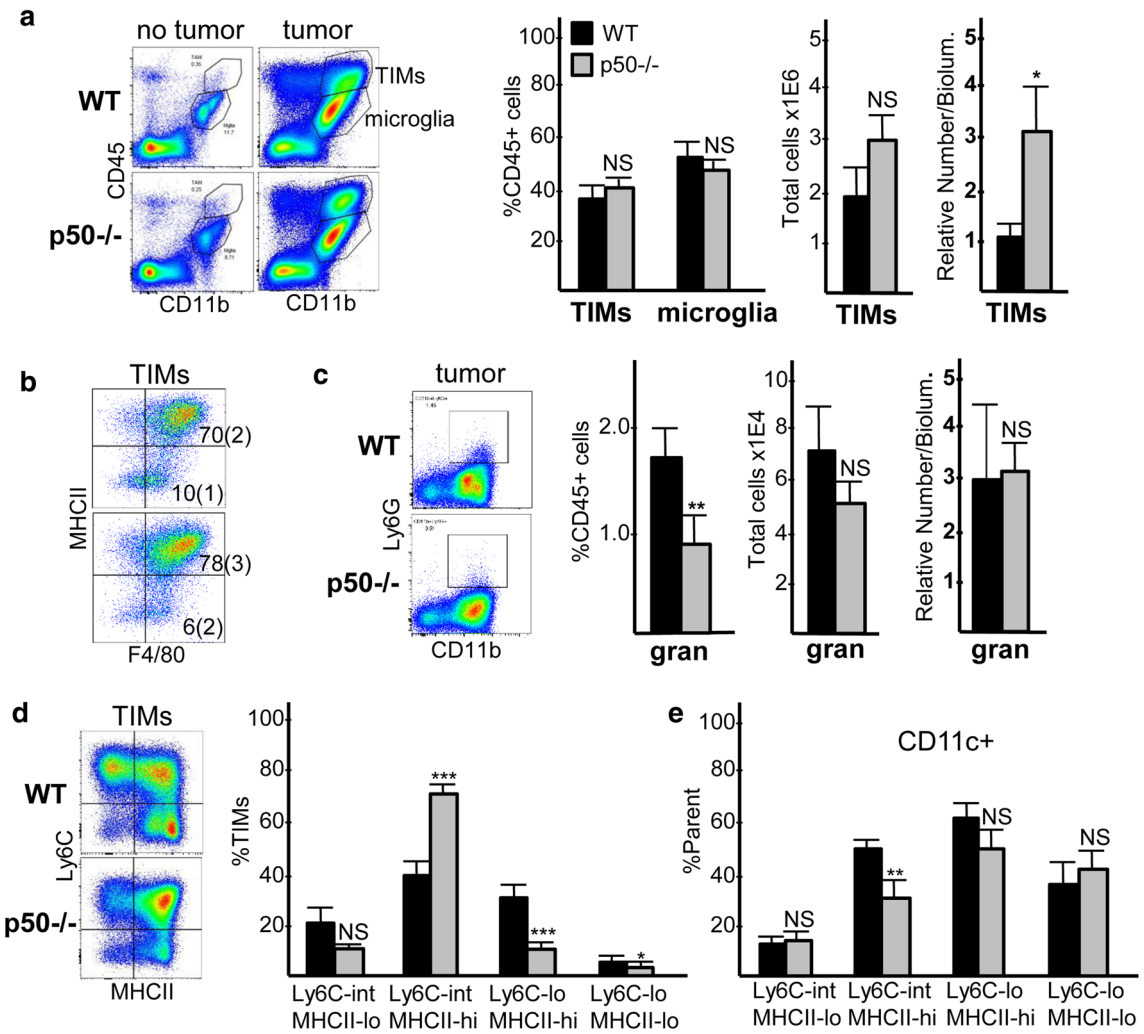

Fig. 2 Characterization of glioma myeloid cells. **a** Representative CD11b;CD45 FC data for brain cells from control and tumor-bearing mice isolated on day 14 after GL261-Luc inoculation, with TIM and microglia populations indicated (left). TIMs and microglia were quantified as a percent of $CD45^+$ cells, and TIMs were also quantified as total number per tumor or by their numbers per bioluminescence upon IVIS imaging, in relative units, as a measure of tumor size (right, mean and SE from ten determinations). **b** Representative MHCII;F4/80 FC data for TIMs, with mean indicated (SE in parenthesis) for the percent of cells in the upper right and lower right quadrants. **c** Representative Ly6G;CD11b plots within tumor $CD45^+$ gate (left). $Ly6G^+$ cells were quantified as percent of $CD45^+$ cells, total number per tumor, and by the number per bioluminescence unit (right, mean and SE from three determinations). **d** Representative Ly6C;MHCII FC plots within the TIM gate (left). The indicated Ly6C;MHCII subsets were quantified as percent of TIMs (right, mean and SE from ten determinations). **e** Percent of each Ly6C;MHCII subset expressing CD11c (mean and SE from four determinations)

We also conducted FC on glioma $CD45^{int}CD11b^{int}$ microglia. On average, 71% of WT and 94% of $p50^{-/-}$ microglia were $F4/80^{hi}$ (Supplementary Fig. 2a). The proportion of WT vs $p50^{-/-}$ microglia expressing MHCII was increased (27 vs 56%, $p = 0.001$) and the proportion expressing MR decreased (14 vs 11%, $p = 0.05$); and only 3% of WT or $p50^{-/-}$ microglia expressed CD11c (Supplementary Fig. 2b).

To evaluate additional polarization markers, we isolated tumor $CD11b^+$ cells 14–16 days after GL261-Luc inoculation and evaluated RNA from these cells by qRT-PCR (Fig. 3c). In $p50^{-/-}$ $CD11b^+$ cells, the M1 macrophage markers *IL-1β, IL-12β, Tnfβ*, and *Nos2* were increased, with a trend towards increased *IL-6*; the M2 markers *Fizz1, MR, Mmp9, Ccl17, Ccl22*, and *Arg* were reduced. M2-associated *Tgfβ* and *IL-10* were not significantly different. Collectively, these FC and qRT-PCR data indicate that $p50^{-/-}$ TIMs and microglia are reprogrammed towards an M1 phenotype. As there is some overlap in tumor sizes at day 14, we were able to directly compare WT and $p50^{-/-}$ TIM in a several tumors of the same size. Compared to WT TIM, the $p50^{-/-}$ TIM maintain increased M1 polarization and increased frequency of their $Ly6C^{int}MHCII^{hi}$ subset, indicating that these changes are not merely a consequence of smaller tumor size (Supplementary Fig. 3).

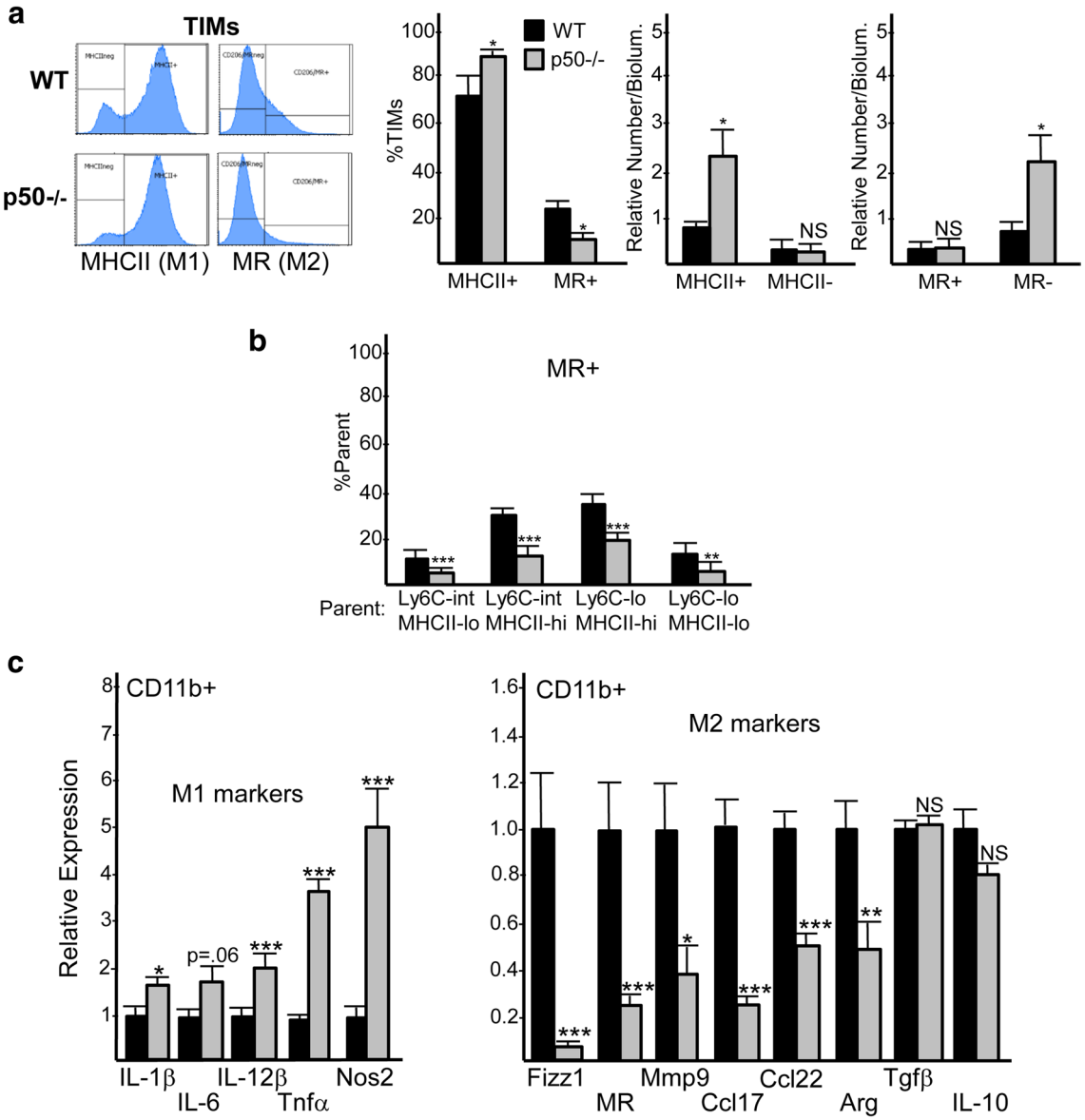

Fig. 3 Glioma myeloid cells have increased M1 markers and decreased M2 markers and express less CD11c in p50$^{-/-}$ recipients. **a** Representative FC plots for expression of MHCII and MR among CD11b^{hi}CD45^{hi} TIMs are shown. MHCII^{+}, MHCII^{-}, MR^{+}, and MR^{-} cells were quantified as percent of TIMs or as the relative number per bioluminescence unit (mean and SE from ten determinations). **b** MR^{+} or CD11c^{+} cells were quantified as the percent of cells within each Ly6C;MHCII quadrant (mean and SE from ten determinations). **c** RNAs prepared from tumor CD11b^{+} cells on day 14 after GL261-Luc inoculation were subjected to qRT-PCR analysis for indicated M1 and M2 markers. The relative expression of each mRNA, normalized to *cyclophilin A*, is shown for WT or p50$^{-/-}$ recipients, with expression in WT mice set to 1.0. Mean and SE are shown for 16 mice total in each group, combined from three separate experiments. *$p<0.05$, **$p<0.01$, ***$p<0.001$

Increased tumor T-cell activation in glioma-bearing NF-κB p50$^{-/-}$ mice

Glioma-bearing WT and p50$^{-/-}$ brains were analyzed by FC for total CD4 and CD8 tumor-infiltrating lymphocytes (TIL) (Fig. 4a, left). CD4 TIL were increased ~threefold in tumors forming in p50$^{-/-}$ mice, both in absolute number and density. CD8 TIL numbers were not significantly changed (Fig. 4a, right). CD4 TIL were the predominant tumor T cell present, being ~twofold greater than CD8 TIL in WT mice, and ~threefold greater than CD8 TIL in p50$^{-/-}$ mice. Of note, in the absence of tumor there were only 10,400 CD4 and 450 CD8 T cells per brain, on average ($n=3$, not shown). CD25^{+}Foxp3^{+} Tregs were reduced ~1.5-fold, as a percent of total CD4 TIL, in p50$^{-/-}$ recipients (Fig. 4b); however, due to the overall increase in the total number

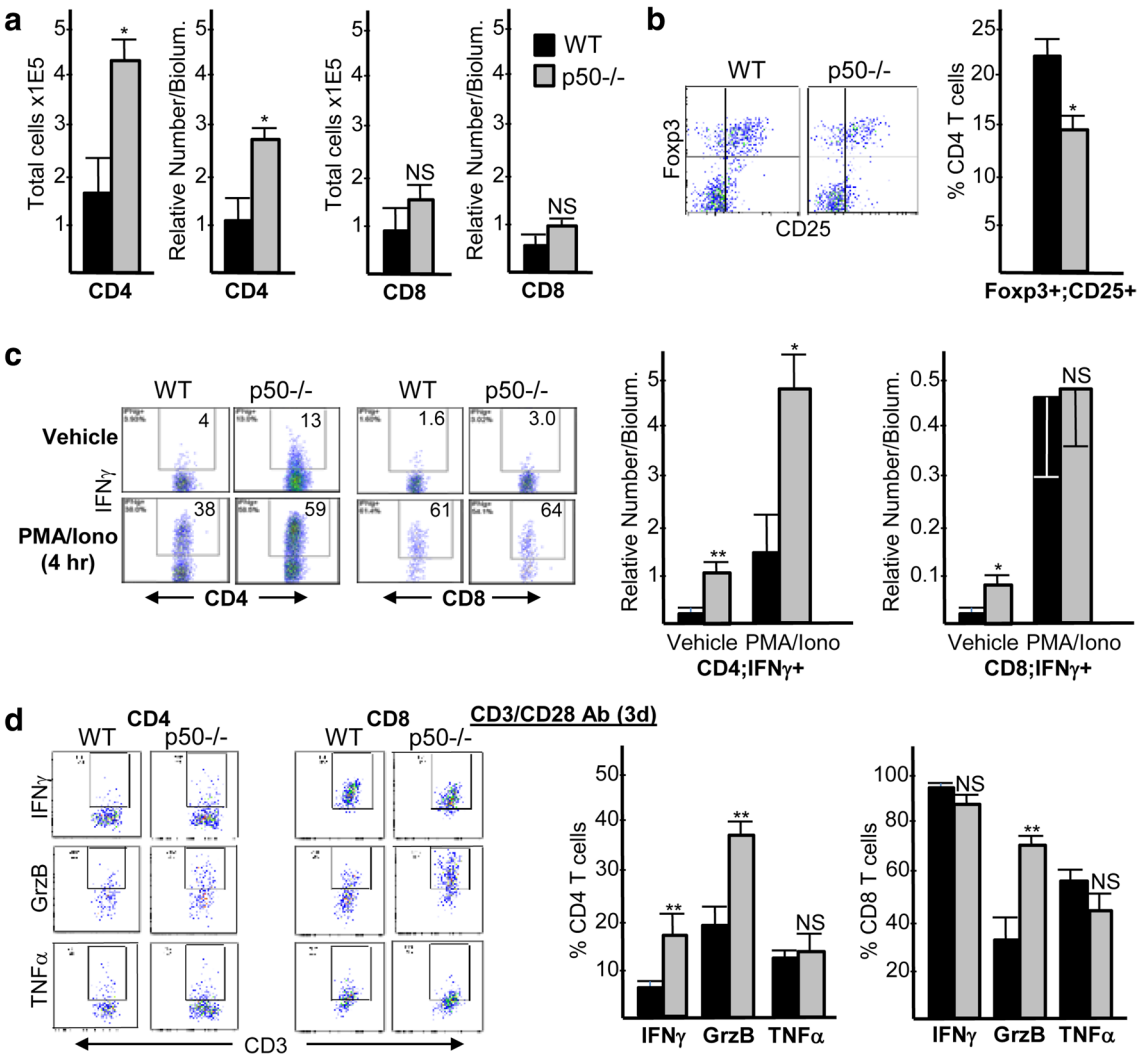

Fig. 4 Gliomas in $p50^{-/-}$ hosts have increased total and activated CD4 T cells and, to a lesser extent, increased activated CD8 T cells. **a** CD4 or CD8 cells were quantified as total number per tumor and the relative number per tumor bioluminescence 14 days after inoculation of GL261-Luc into WT or $p50^{-/-}$ mice (mean and SE from four determinations). **b** Representative Foxp3;CD25 FC plots within the $CD3^+CD4^+$ T-cell subset (left) and quantification of $Foxp3^+CD25^+$ Tregs as a percent of CD4 cells (right, mean and SE from four determinations) are shown. **c** Representative CD4;IFNγ and CD8;IFNγ FC plots, within the $CD3^+$ T-cell gate, are shown 4 h after exposure to vehicle or PMA/ionomycin (left). $CD4^+IFN\gamma^+$ or $CD8^+IFN\gamma^+$ cells were quantified as the relative number per bioluminescence unit (right, mean and SE from four determinations). **d** Representative CD3;IFNγ, CD3;Granzyme B (GrzB), and CD3;TNFα FC plots, within $CD4^+$ or $CD8^+$ gates, are shown 3 days after stimulation of isolated $CD3^+$ tumor cells with Dynabeads containing CD3 and CD28 antibodies (left). $IFN\gamma^+$, $GrzB^+$, and $TNF\alpha^+$ cells were quantified as percent of $CD4^+$ or $CD8^+$ cells (right, mean and SE from five determinations)

of CD4 TIL in $p50^{-/-}$ mice, total numbers of Tregs were unchanged and Treg density was increased in the absence of p50 (Supplementary Fig. 4a).

Intracellular IFNγ expression, a marker of T-cell activation, was assessed in TIL after 4 h exposure to PMA/ionomycin or vehicle (Fig. 4c). In $p50^{-/-}$ mice, IFNγ expression was increased in vehicle-treated CD4 and CD8 TIL, as well as in stimulated CD4 TIL. Notably, the density of vehicle-treated IFNγ-expressing CD4 TIL was 10-fold higher than that of CD8 TIL in $p50^{-/-}$ recipients, and ~threefold greater in absolute number. Designating IFNγ-expressing T cells as T effectors, the $p50^{-/-}$ Treg:CD4 effector ratio was reduced 10-fold in vehicle-treated and threefold in PMA/ionomycin-treated cells as compared to WT ratios. The $p50^{-/-}$ Treg:CD8 effector ratio was reduced twofold in vehicle-treated cells and was slightly increased in PMA/ionomycin-treated cells (Supplementary Fig. 4b). Intracellular IFNγ Granzyme B, and TNFα expression were also assessed in TIL after 3 days of ex vivo stimulation with CD3/CD28 antibodies (Fig. 4d). $p50^{-/-}$ CD4

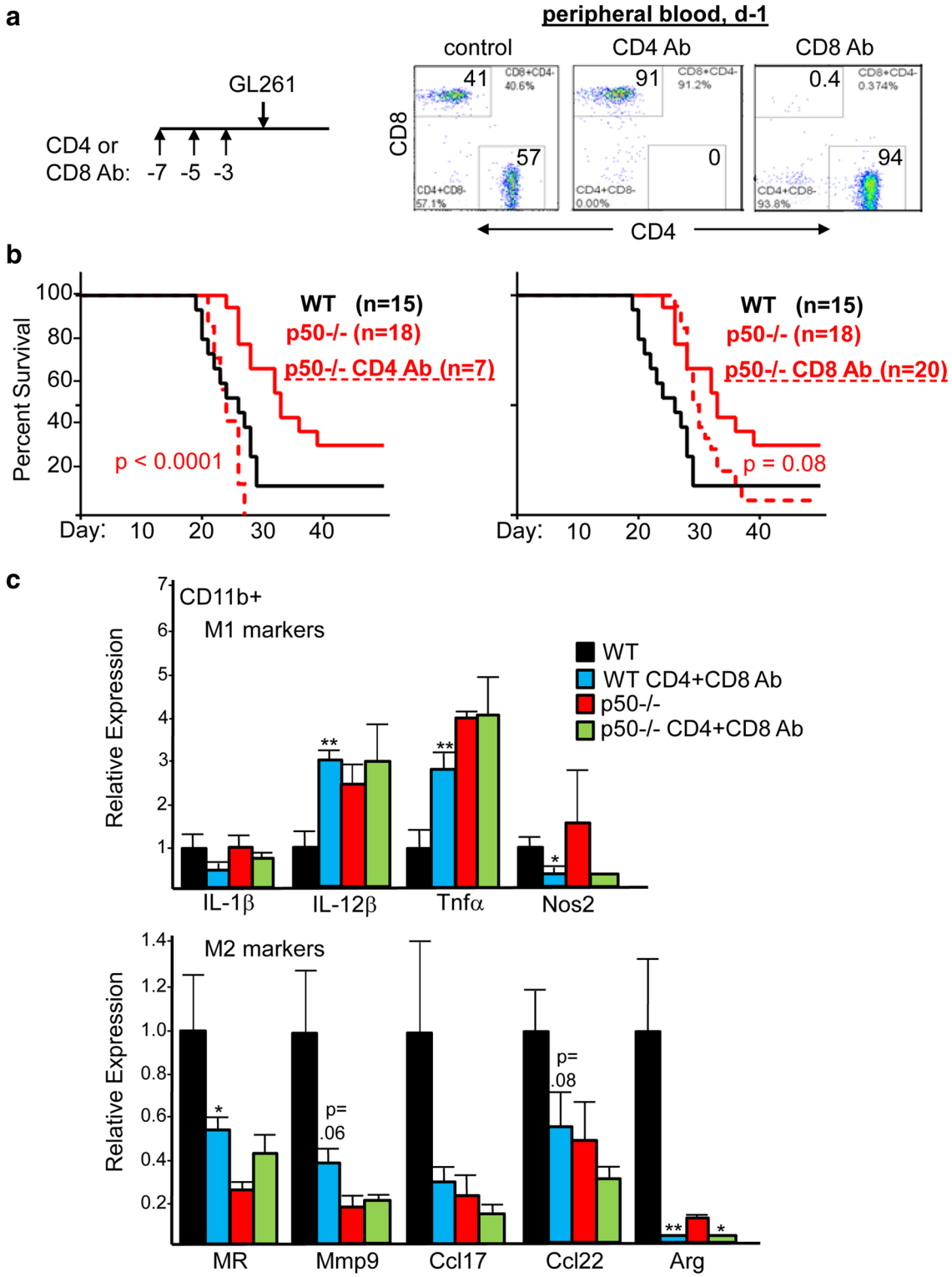

TIL had increased IFNγ and Granzyme B, and p50$^{-/-}$ CD8 TIL also had increased Granzyme B. Thus, compared with WT mice, tumors from p50$^{-/-}$ mice possess elevated numbers of CD4 TIL that exhibit a more activated, anti-tumor phenotype at baseline and upon stimulation. CD8 TIL are also more activated in p50$^{-/-}$ mice at baseline, albeit at lower numbers.

To evaluate the cell-intrinsic impact of p50 deletion in T cells, we isolated naïve splenic CD4 T cells or CD8 T cells from WT and p50$^{-/-}$ mice and cultured them under

◂**Fig. 5** Survival advantage of $p50^{-/-}$ mice is eliminated by depletion of CD4 T cells and partially eliminated by CD8 depletion, and combined CD4 and CD8 depletion reverses WT tumor myeloid M2 polarization. **a** WT and $p50^{-/-}$ mice received 200 µg CD4 or CD8 antibody (Ab) on days 7, 5, and 3, followed by GL261-Luc cell inoculation on d0, as diagrammed (left). Representative CD4;CD8 FC plots demonstrating efficient depletion of CD4 or CD8 T cells from the peripheral blood 1 day prior to GL261 inoculation (right). **b** Survival curves for glioma-bearing WT mice, $p50^{-/-}$ mice, or $p50^{-/-}$ mice pre-treated with CD4 or CD8 Ab. The number of mice in each group and Log Rank *p* values comparing the control and Ab-treated $p50^{-/-}$ groups are shown. The untreated WT and $p50^{-/-}$ mice in this experiment are a subset of those presented in Fig. 1 and were inoculated concurrently with those exposed to the T-cell-depleting Abs. **c** WT and $p50^{-/-}$ mice received both CD4 and CD8 antibody (Ab), or no Ab, on days -7, -5, and -3, followed by GL261-Luc cell inoculation on d0 and an additional CD4/CD8 Ab injection on d8. $CD11b^{+}$ cells isolated on day 14 were subjected to qRT-PCR analysis for indicated mRNAs (mean and SE from three determinations)

conditions that favor differentiation into several CD4 subsets or the CD8 Tc1 subset. Evaluation of intracellular IFNγ, Foxp3, and IL-17 expression indicated that $p50^{-/-}$ CD4 T cells possess no defect in their ability to become Th1, Treg, or Th17 cells. IL-4 secretion was unchanged in $p50^{-/-}$ CD4 T cells differentiated into the Th2 subset (Supplementary Fig. 5a). In contrast, CD8 Tc1 formation was increased in the absence of p50, indicated by elevated proportions of CD8 T cells expressing IFNγ, Granzyme B, and TNFα (Supplementary Fig. 5b). Lack of increased IFNγ or TNFα in tumor CD8 $p50^{-/-}$ T cells cultured with CD3/CD28 may reflect their alteration by the tumor or limitations of this ex vivo assay.

T-cell depletion eliminates the survival benefit of $p50^{-/-}$ and reverses M2 polarization in WT hosts

To remove T cells, mice received three doses of CD4 or CD8 antibody 7, 5, and 3 days prior to GL261-Luc implantation; depletion was confirmed by analysis of peripheral blood 1 day prior to implantation (Fig. 5a). CD4 antibody fully obviated the survival advantage of $p50^{-/-}$ mice, whereas CD8 antibody reduced, but did not eliminate, this advantage (Fig. 5b). CD8 T cells recovered to 3% of peripheral blood cells by day 19, on average, compared to 18% at baseline (not shown), potentially reducing the effect of CD8 depletion on survival. Neither CD4 nor CD8 antibody affected the survival of WT mice (Supplementary Fig. 6).

To evaluate TIM polarization in the absence of T cells, we pre-depleted CD4 and CD8 cells, inoculated mice with GL261-Luc, and then isolated brain $CD11b^{+}$ cells on day 14. We evaluated M1 and M2 markers by qRT-PCR, focusing on those markers that differed without depletion (Fig. 5c). Strikingly, T-cell depletion in WT mice increased *IL-12β* and *TNFα* (M1) and decreased *MR, Mmp9, Ccl17, Ccl22*, and *Arg* (M2) to levels seen in untreated $p50^{-/-}$ mice. In contrast, T-cell depletion of $p50^{-/-}$ mice had little effect on these mRNAs, with the exception of *Arg*. T-cell depletion did not increase the expression of *IL-1β* or *Nos2* in WT mice. The lack of prolonged survival in WT mice depleted of CD4 or CD8 T cells suggests that the resulting M2-to-M1 shift in TIM is not as strong as that resulting from p50 gene deletion.

Deletion of neutrophil/macrophage NF-κB p50 does not slow glioma growth

$p50(f^{lacZ}/+)$ mice, harboring a floxed *p50* exon 4 with an intron 3 l*ac*Z cassette flanked by *frt* sites, were bred with ROSA26-FLPo and then Lysozyme-Cre to generate p50(f/f) and p50(f/f);Lys-Cre mice. Lys-Cre deletes floxed alleles in activated monocytes, macrophages, and granulocytes [33]. Efficient Lys-Cre-mediated deletion of exon 4 was evident upon PCR of BMDM genomic DNA (Fig. 6a, left), resulting in markedly reduced p50 RNA and protein in BMDM at baseline and after stimulation with IL-4 or IFNγ (Fig. 6a, center and right). The p105 precursor of p50 was also reduced. Efficient deletion was also evident in peritoneal macrophages (Fig. 6b). Survival of p50(f/f) or p50(f/f);Lys-Cre mice inoculated with GL261-Luc glioma cells was essentially identical, with tumor growth also unaffected by reduced myeloid p50 (Fig. 6c). Analysis of tumor $CD11b^{+}$ cell RNA reveals a trend towards increased *Nos2* and T*NFα* (M1), as well as reduced *Ccl17* with a trend towards reduced *Ccl22* (M2); in contrast to $p50^{-/-}$ tumor hosts, *Fizz1, MR, Mmp9*, and *Arg* (M2) were not reduced in p50(f/f);Lys-Cre mice (Fig. 6d). Lack of slowed tumor growth and prolonged survival in p50(f/f);Lys-Cre mice may in part reflect poor *p50* exon 4 deletion in microglia. Microglial deletion of exon 4 was evaluated by analysis of RNA in brain $CD11b^{+}$ cells from tumor-free mice, and also in sorted $CD11b^{int}CD45^{int}$ cells from tumor-bearing mice, in comparison to $CD11b^{hi}CD45^{hi}$ TIMs (Fig. 6e). p50 RNA was decreased 80% in TIMs, only 20% in naïve microglia, and 50% in tumor-associated microglia, the latter potentially an underestimate due to inclusion of non-tumor microglia.

Discussion

GL261 gliomas grew substantially slower in $p50^{-/-}$ compared with WT hosts. Tumor regression was evident after day 14 in 30% of $p50^{-/-}$ recipients, suggesting effective immune surveillance resulting in prolonged survival. Of note, GL261 cells carry a high mutational burden and express > 1700 neoepitopes [34].

Gliomas in WT and $p50^{-/-}$ mice contained a large population of $CD45^{hi}CD11b^{hi}$ cells. Both TAMs and MDSC have been identified in tumors and support tumor growth. MDSC are immature myeloid cells that can be either granulocytic ($Ly6G^{hi}$) or monocytic ($Ly6C^{hi}$), both of which are

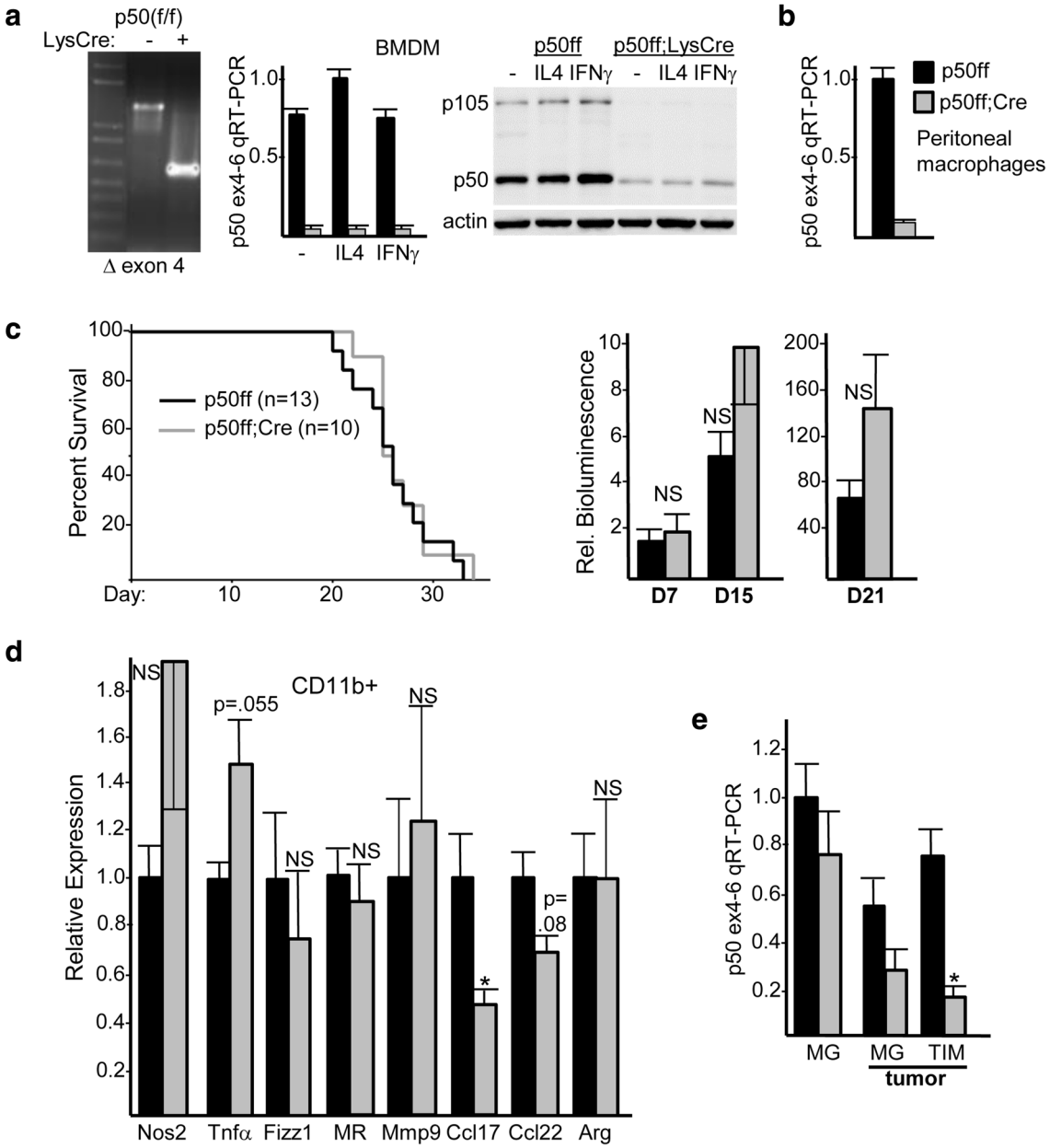

Fig. 6 Glioma growth is not slowed in mice lacking myeloid NF-κB p50. **a** PCR analysis of genomic DNA from p50(f/f) and p50(f/f);Lys-Cre mice (left). RNA isolated from BMDM under basal conditions in CSF1 or after stimulation for 24 h with IL-4 (M2 inducer) or IFNγ (M1 inducer) was analyzed by qRT-PCR using p50 exon 4 and exon 6 primers (center, mean and SE from three determinations); total cellular proteins from the same cultures were analyzed by Western blotting for p50 and β-actin (right). **b** Peritoneal macrophages from p50(f/f) and p50(f/f);Lys-Cre mice were analyzed for *p50* RNA by exon 4–6 qRT-PCR (mean and SE from three determinations). **c** Survival curves of p50(f/f) vs p50(f/f);Lys-Cre mice inoculated on day 0 with GL261-Luc cells, with total number of mice in each group and Log Rank *p* values shown (left). Relative IVIS bioluminescence of tumors on days 7, 15, and 21 from the same mice used for survival analysis (right). **d** RNAs prepared from tumor CD11b$^+$ cells on day 14 after GL261-Luc inoculation were subjected to qRT-PCR analysis for indicated M1 and M2 markers. The relative expression of each mRNA, normalized to *cyclophilin A*, is shown, with expression in p50(f/f) mice set to 1.0. Mean and SE are shown for three mice per group. **e** p50 RNA expressed was evaluated by exon 4–6 qRT-PCR in microglia (MG) from tumor-free mice and in MG and TIMs sorted from tumors 14 days after GL261 inoculation (mean and SE from three determinations)

characterized by low or absent F4/80 and MHCII [7, 35]. We found that the majority of CD45^{hi}CD11b^{hi} cells were F4/80^{hi} TAMs in both WT and p50$^{-/-}$ mice, and only a small proportion expressed Ly6G. Although we observed a large proportion of p50$^{-/-}$ TIMs expressing intermediate Ly6C, these cells co-expressed high levels of both F4/80 and

MHCII, ruling out the possibility that they are suppressive monocytic MDSC. Thus, the glioma-infiltrating myeloid cells in this model are predominantly TAMs and microglia.

When normalized to tumor bioluminescence, we found a threefold increase in TIM density in $p50^{-/-}$ mice. Evaluation of surface markers confirmed that $p50^{-/-}$ TIMs express less MR and more MHCII, consistent with the partial M2-to-M1 phenotypic shift found via mRNA analysis of $CD11b^{+}$ cells. Interestingly, a similar increase in MHCII and decrease in MR was seen in $CD45^{int}CD11b^{int}$ microglia. The $Ly6C^{int}MHCII^{hi}$ TIM subset was increased in $p50^{-/-}$ mice which, together with M2-to-M1 reprogramming, correlates with reduced growth of gliomas and other tumors [1, 11, 31]. TNFα- and Nos2-producing inflammatory dendritic cells (Tip-DCs) have recently been identified within the $Ly6C^{int}MHCII^{hi}$ population [31]. Although $p50^{-/-}$ $CD11b^{+}$ cells have increased *Tnf*α and *Nos2* mRNA expression, we observe reduced CD11c within the $Ly6C^{int}MHCII^{hi}$ subset of $p50^{-/-}$ TIMs, which is inconsistent with a Tip-DC identity. Reduced CD11c expression in tumor-bearing $p50^{-/-}$ mice is consistent with the finding that $F4/80^{hi}CD11c^{hi}$ TAMs increase glioma growth upon intracranial co-inoculation into NOD/SCID mice [32]. Supporting the idea that myeloid NF-κB activation in the absence of p50 contributes to glioma control, inhibition of myeloid-specific PI3Kγ induces TAMs to adopt an M1 phenotype, with increased NF-κB p65 activity and slowed growth of several murine carcinoma lines [36].

Potentially as a consequence of the observed changes in tumor myeloid cells, we discovered a marked increase in total and IFNγ-expressing CD4 TIL in $p50^{-/-}$ mice, which outnumbered total and activated CD8 TIL threefold in absolute number, and 10-fold in density. Stimulation with PMA/ionomycin increased IFNγ expression in a greater proportion of CD4 TIL from $p50^{-/-}$ mice than WT mice. Upon stimulation for 3 days ex vivo using CD3/CD28 antibodies, we detected increased Granzyme B in CD8 TIL, and increased Granzyme B, IFNγ, and TNFα in CD4 TIL from $p50^{-/-}$ hosts. We detected no change in *Tgfb* mRNA expression in $p50^{-/-}$ $CD11b^{+}$ cells, which correlates with unaltered total numbers of tumor Tregs. However, when increased numbers of $IFN\gamma^{+}$ CD4 T cells are taken into account, we find a 10-fold decrease in the ratio of Treg:CD4 effectors in tumors from $p50^{-/-}$ mice. We find a similar trend, albeit a lower twofold change, in the Treg:CD8 effector ratio. Collectively, our T-cell data suggest a greater relevance of CD4 T-cell activation than CD8 T-cell activation for reducing GL261 glioma growth and prolonging survival in the absence of p50. The crucial role of CD4 T cells in controlling brain tumor growth has been seen in the GL261 model upon immune checkpoint blockade and in a medulloblastoma model upon tumor Cdk5 kinase loss that results in reduced tumor PD-L1 [37, 38]. In the clinical setting, low CD4 counts have been correlated with increased tumor growth and earlier death in glioma patients [39, 40].

The contribution of CD4 and CD8 T cells to slowed tumor growth in $p50^{-/-}$ hosts was evident from the complete ablation of survival advantage upon CD4 T-cell depletion, and from partial ablation of survival advantage upon CD8 T-cell depletion. CD8 T-cell activation was at least in part cell-intrinsic, as cultured naïve splenic $p50^{-/-}$ CD8 T cells gave rise to increase Tc1 cells. Although ex vivo naïve splenic $p50^{-/-}$ CD4 T-cell skewing to Th1, Th2, Th17, or Treg phenotypes was equivalent to that of WT cells, we cannot rule out a cell-intrinsic effect of p50 deletion on tumor CD4 Th1 activation in vivo.

Two additional findings support a role for T-cell-intrinsic changes in the absence of p50 contributing to slowed glioma growth in $p50^{-/-}$ mice. First, combined CD4 and CD8 T-cell ablation largely reversed tumor myeloid M2 polarization in WT hosts without affecting tumor myeloid M1 polarization in $p50^{-/-}$ hosts. To our knowledge, these data reveal a largely unappreciated role for T cells in maintaining tumor-supportive TAM M2 polarization. The M1 markers *IL-1β* and *Nos2* were not increased in WT hosts upon T-cell depletion, suggesting that their increase in $p50^{-/-}$ tumor myeloid cells may result from a myeloid cell-intrinsic change. Second, glioma growth was not slowed in p50(f/f);Lys-Cre compared with p50(f/f) tumor recipients. Future experiments will utilize additional Cre transgenes, e.g., CD4-Cre, CD8α-Cre, CD11c-Cre, or combinations, to further dissect the relevant cell types.

Collectively, our findings suggest that targeting NF-κB p50 in both tumor T cells and myeloid cells has the potential to contribute to glioma therapy. Although targeting the p50 protein may be problematic, using a p50 siRNA directed to these cells in vivo represents a viable therapeutic option. Depleting p50 in T cells may both obviate their ability to induce tumor myeloid M2 polarization and directly favor their activation by tumor antigens, whereas depleting myeloid p50 may directly enable their adoption of an anti-tumor M1 phenotype. Importantly, inactivation of the NF-κB p50 transcription factor could potentially avoid resistance mechanisms that arise when upstream, cytoplasmic signaling pathways are targeted.

Author contributions TB, AM, RS, DJB, and SH-B conducted experiments. CGD, ML, and ADF guided the conduct of experiments. TB and ADF wrote the manuscript.

Funding This study was supported by grants from Alex's Lemonade Stand Foundation, Hyundai Hope on Wheels, the Allegheny Health Network-Johns Hopkins Cancer Research Fund, the National Institutes of Health (T32 CA60441 and P30 CA006973), and by the Giant Food Children's Cancer Research Fund.

Compliance with ethical standards

Conflict of interest The authors declare that they have no conflict of interest.

Ethical approval and ethical standards All applicable international, national, and/or institutional guidelines for the care and use of animals were followed. All procedures performed in studies involving animals were in accordance with the ethical standards of the institution or practice at which the studies were conducted.

Animal source WT C57BL/6 (B6) mice were obtained from Charles River Laboratories, *Nfkb1*(p50)$^{-/-}$, Lys-Cre, and ROSA26-FLPo mice from Jackson Laboratory (6097, 4781, 12930), and p50(f^{lacZ}/+) mice from the Knockout Mouse Project (CSD29053).

Cell line authentication GL261-Luc cells were obtained from Perkin Elmer, who had authenticated it as C57BL/6 in origin by mouse STR analysis.

References

1. Kennedy BC, Showers CR, Anderson DE, Anderson L, Canoll P, Bruce JN, Anderson SC (2013) Tumor-associated macrophages in glioma: friend or foe? J Oncol 2013:486912
2. Gabrusiewicz K, Ellert-Miklaszewska A, Lipko M, Sielska M, Frankowska M, Kaminska B (2011) Characteristics of the alternative phenotype of microglia/macrophages and its modulation in experimental gliomas. PLoS One 6:e23902
3. Ginhoux F, Greter M, Leboeuf M, Nandi S, See P, Gokhan S, Mehler MF, Conway SJ, Ng LG, Stanley ER, Samokhvalov IM, Merad M (2010) Fate mapping analysis reveals that adult microglia derive from primitive macrophages. Science 330:841–845
4. Shand FH, Ueha S, Otsuji M, Koid SS, Shichino S, Tsukui T, Kosugi-Kanaya M, Abe J, Tomura M, Ziogas J, Matsushima K (2014) Tracking intertissue migration reveals the origins of tumor-infiltrating monocytes. Proc Natl Acad Sci USA 111:7771–7776
5. Sica A, Bronte V (2007) Altered macrophage differentiation and immune dysfunction in tumor development. J Clin Invest 117:1155–1166
6. Mosser DM, Edwards JP (2008) Exploring the full spectrum of macrophage activation. Nat Rev Immunol 8:958
7. Gabrilovich DI, Ostrand-Rosenberg S, Bronte V (2012) Coordinated regulation of myeloid cells by tumours. Nat Rev Immunol 12:253–268
8. Franklin RA, Liao W, Sarkar A, Kim MV, Bivona MR, Liu K, Pamer EG, Li MO (2014) The cellular and molecular origin of tumor-associated macrophages. Science 344:921–925
9. Noy R, Pollard JW (2014) Tumor-associated macrophages: from mechanisms to therapy. Immunity 41:49–61
10. Li W, Graeber MB (2012) The molecular profile of microglia under the influence of glioma. Neuro Oncol 14:958–978
11. Pyonteck SM, Akkari L, Schuhmacher AJ, Bowman RL, Sevenich L, Quail DF, Olson OC, Quick ML, Huse JT, Teijeiro V, Setty M, Leslie CS, Oei Y, Pedraza A, Zhang J, Brennan CW, Sutton JC, Holland EC, Daniel D, Joyce JA (2013) CSF-1R inhibition alters macrophage polarization and blocks glioma progression. Nature Med 19:1264–1272
12. Sielska M, Przanowski P, Wylot B, Gabrusiewicz K, Maleszewska M, Kijewska M, Zawadzka M, Kucharska J, Vinnakota K, Kettenmann H, Kotulska K, Grajkowska W, Kaminska B (2013) Distinct roles of CSF family cytokines in macrophage infiltration and activation in glioma progression and injury response. J Pathol 230:310–321
13. Quail DF, Bowman RL, Akkari L, Quick ML, Schuhmacher AJ, Huse JT, Holland EC, Sutton JC, Joyce JA (2016) The tumor microenvironment underlies acquired resistance to CSF-1R inhibition in gliomas. Science 352:aad3018
14. Bohuslav J, Kravchenko VV, Parry GC, Erlich JH, Gerondakis S, Mackman N, Ulevitch RJ (1998) Regulation of an essential innate immune response by the p50 subunit of NF-κB. J Clin Invest 102:1645–1652
15. Saccani A, Schioppa T, Porta C, Biswas SK, Nebuloni M, Vago L, Bottazzi B, Colombo MP, Mantovani A, Sica A (2006) p50 nuclear factor-kB overexpression in tumor-associated macrophages inhibits M1 inflammatory responses and antitumor resistance. Cancer Res 66:11432–11440
16. Porta C, Rimoldi M, Raes G, Brys L, Ghezzi P, Di Liberto D, Dieli F, Ghisletti S, Natoli G, De Baetselier P, Mantovani A, Sica A (2009) Tolerance and M2 (alternative) macrophage polarization are related processes orchestrated by p50 nuclear factor kB. Proc Natl Acad Sci USA 106:14978–14983
17. Kono Y, Kawakami S, Higuchi Y, Yamashita F, Hashida M (2014) In vitro evaluation of inhibitory effect of nuclear factor-κB activity by small interfering RNA on pro-tumor characteristics of M2-like macrophages. Biol Pharm Bull 37:137–144
18. Rackov G, Hernandez-Jimenez E, Shokri R, Carmona-Rodríguez L, Mañes S, Álvarez-Mon M, López-Collazo E, Martínez-A C, Balomenos D (2016) p21 mediates macrophage reprogramming through regulation of p50–p50 NF-κB and IFN-β. J Clin Invest 126:3089–3103
19. Ruffell D, Mourkioti F, Gambardella A, Kirstetter P, Lopez RG, Rosenthal N, Nerlov C (2009) A CREB-C/EBPβ cascade induces M2 macrophage-specific gene expression and promotes muscle injury repair. Proc Natl Acad Sci USA 106:17475–17480
20. Marigo I, Bosio E, Solito S, Mesa C, Fernandez A, Dolcetti L, Ugel S, Sonda N, Bicciato S, Falisi E, Calabrese F, Basso G, Zanovello P, Cozzi E, Mandruzzato S, Bronte V (2010) Tumor-induced tolerance and immune suppression depend on the C/EBPβ transcription factor. Immunity 32:790–802
21. Feinberg MW, Wara AK, Cao Z, Lebedeva MA, Rosenbauer F, Iwasaki H, Hirai H, Katz JP, Haspel RL, Gray S, Akashi K, Segre J, Kaestner KH, Tenen DG, Jain MK (2007) The Kruppel-like factor KLF4 is a critical regulator of monocyte differentiation. EMBO J 26:4138–4148
22. Tugal D, Liao X, Jain MK (2013) Transcriptional control of macrophage polarization. Arterioscler Thromb Vasc Biol 33:1135–1144
23. Strauss L, Sangaletti S, Consonni FM, Szebeni G, Morlacchi S, Totaro MG, Porta C, Anselmo A, Tartari S, Doni A, Zitelli F, Tripodo C, Colombo MP, Sica A (2015) RORC1 regulates tumor-promoting "emergency" granulo-monocytopoiesis. Cancer Cell 28:253–269
24. Newcomb EW, Zagzag D (2009) The murine GL261 glioma experimental model to assess novel brain tumor treatments. In: Van Meir EG (ed) CNS cancer, models, markers, prognostic factors, targets, and therapeutic approaches. Humana Press, New York, pp 228–241
25. Zeng J, See AP, Phallen J, Jackson CM, Belcaid Z, Ruzevick J, Durham N, Meyer C, Harris TJ, Albesiano E, Pradilla G, Ford E, Wong J, Hammers HJ, Mathios D, Tyler B, Brem H, Tran PT, Pardoll D, Drake CG, Lim M (2013) Anti-PD-1 blockade and stereotactic radiation produces long term survivors in mice with intracranial glioma. Int J Radiat Oncol Biol Phys 86:343–349
26. Flaherty S, Reynolds JM (2015) Mouse naïve CD4+ T cell isolation and in vitro differentiation into T cell subsets. J Vis Exp 98:52739

27. Badie B, Schartner JM (2000) Flow cytometric characterization of tumor-associated macrophages in experimental gliomas. Neurosurgery 46:957–961
28. Movahedi K, Laoui D, Gysemans C, Baeten M, Stangé G, Van den Bossche J, Mack M, Pipeleers D, In't Veld P, De Baetselier P, Van Ginderachter JA (2010) Different tumor microenvironments contain functionally distinct subsets of macrophages derived from Ly6C(high) monocytes. Cancer Res 70:5728–5739
29. Georgoudaki AM, Prokopec KE, Boura VF, Hellqvist E, Sohn S, Östling J, Dahan R, Harris RA, Rantalainen M, Klevebring D, Sund M, Brage SE, Fuxe J, Rolny C, Li F, Ravetch JV, Karlsson MC (2016) Reprogramming tumor-associated macrophages by antibody targeting inhibits cancer progression and metastasis. Cell Rep 15:2000–2011
30. Muller A, Brandenburg S, Turkowski K, Muller S, Vajkoczy (2015) Resident microglia, and not peripheral macrophages, are the main source of brain tumor mononuclear cells. Int J Cancer 137:278–288
31. Marigo I, Zilio S, Desantis G, Mlecnik B, Agnellini AH, Ugel S, Sasso MS, Qualls JE, Kratochvill F, Zanovello P, Molon B, Ries CH, Runza V, Hoves S, Bilocq AM, Bindea G, Mazza EM, Bicciato S, Galon J, Murray PJ, Bronte V (2016) T cell cancer therapy requires CD40-40L activation of tumor necrosis factor and inducible nitric-oxide-synthase-producing dendritic cells. Cancer Cell 30:377–390
32. Kokubu Y, Tabu K, Muramatsu N, Wang W, Murota Y, Nobuhisa I, Jinushi M, Taga T (2016) Induction of protumoral CD11c(high) macrophages by glioma cancer stem cells through GM-CSF. Genes Cells 21:241–251
33. Abram CL, Roberge GL, Hu Y, Lowell CA (2014) Comparative analysis of the efficiency and specificity of myeloid-Cre deleting strains using ROSA-EYFP reporter mice. J Immunol Methods 408:89–100
34. Johanns TM, Ward JP, Miller CA, Wilson C, Kobayashi DK, Bender D, Fu Y, Alexandrov A, Mardis ER, Artyomov MN, Schreiber RD, Dunn GP (2016) Endogenous neoantigen-specific CD8 T cells identified in two glioblastoma models using a cancer immunogenomics approach. Cancer Immunol Res 4:1007–1015
35. Gabrilovich DI, Nagaraj S (2009) Myeloid-derived-suppressor cells as regulators of the immune system. Nat Rev Immunol 9:162–174
36. Kaneda MM, Messer KS, Ralainirina N, Li H, Leem CJ, Gorjestani S, Woo G, Nguyen AV, Figueiredo CC, Foubert P, Schmid MC, Pink M, Winkler DG, Rausch M, Palombella VJ, Kutok J, McGovern K, Frazer KA, Wu X, Karin M, Sasik R, Cohen EE, Varner JA (2016) PI3Kγ is a molecular switch that controls immune suppression. Nature 539:437–442
37. Belcaid Z, Phallen JA, Zeng J, See AP, Mathios D, Gottschalk C, Nicholas S, Kellett M, Ruzevick J, Jackson C, Albesiano E, Durham NM, Ye X, Tran PT, Tyler B, Wong JW, Brem H, Pardoll DM, Drake CG, Lim M (2014) Focal radiation therapy combined with 4-1BB activation and CTLA-4 blockade yields long-term survival and a protective antigen-specific memory response in a murine glioma model. PLoS One 9:e101764
38. Dorand RD, Nthale J, Myers JT, Barkauskas DS, Avril S, Chirieleison SM, Pareek TK, Abbott DW, Stearns DS, Letterio JJ, Huang AY, Petrosiute A (2016) Cdk5 disruption attenuates tumor PD-L1 expression and promotes antitumor immunity. Science 353:399–403
39. Ellsworth S, Balmanoukian A, Kos F, Nirschl CJ, Nirschl TR, Grossman SA, Luznik L, Drake CG (2014) Sustained CD4+ T cell-driven lymphopenia without a compensatory IL-7/IL-15 response among high-grade glioma patients treated with radiation and temozolomide. Oncoimmunology 3:e27357
40. Grossman SA, Ye X, Lesser G, Sloan A, Carraway H, Desideri S, Piantadosi S, NABTT CNS Consortium (2011) Immunosuppression in patients with high-grade gliomas treated with radiation and temozolomide. Clin Cancer Res 17:5473–5480